Supplement to "Informing policy via dynamic models: Eliminating cholera in Haiti"

Jesse Wheeler, Anna Rosengart, Zhuoxun Jiang,
Kevin Hao En Tan, Noah Treutle, Edward L. Ionides

Department of Statistics, University of Michigan

October 12, 2022

Supplementary Content

S1   Markov chain and differential equation interpretations of compartment flow rates

In Sections 2.1, 2.2 and 2.3 of the main article, we define compartment models in terms of their flow rates. For a discrete population model, these rates define a Markov chain. For a continuous and deterministic model, the rates define a system of ordinary differential equations. Here, we add additional details to clarify the mapping from a collection of rate functions to a fully specified process. Our treatment follows Bretó et al. (2009).

A general compartment model is a vector-valued process $X(t) = (X_1(t), \ldots, X_c(t))$ denoting the (integer or real-valued) counts in each of c compartments. The compartments may also have names, but to set up general notation we simply refer to them by their numerical index. The basic characteristic of a compartment model is that $X(t)$ can be written in terms of the flows $N_{ij}(t)$ from i to j, together with flows into and out of each compartment denoted by $N_{\bullet i}(t)$ and $N_{i \bullet}(t)$ respectively. These flows are required to satisfy a "conservation of mass" identity:

$$X_i(t) = X_i(0) + N_{\bullet i}(t) - N_{i \bullet}(t) + \sum_{j \neq i} N_{ji}(t) - \sum_{j \neq i} N_{ij}(t). \tag{S1}$$

Each *flow* $N_{ij}(t)$ is associated with a *rate* function $\mu_{ij} = \mu_{ij}(t, X(t))$, where we include the possibility that i or j takes value $\bullet$.

There are different ways to use a collection of rate functions to build a fully specified model. We proceed to describe the ones we use in this paper: via a system of ordinary differential equations (Sec. S1.1), a simple Markov counting system (Sec. S1.2), and an overdispersed Markov counting system (Sec. S1.3). Other representations include stochastic differential equations driven by Gaussian noise or Gamma noise (Bhadra et al., 2011).

S1.1   Ordinary differential equation (ODE) interpretation

A basic deterministic specification is

$$dN_{ij}/dt = \mu_{ij}\big(t, X(t)\big) X_i(t), \quad i \in 1{:}c, \quad j \in 1{:}c \cup \{\bullet\}, \quad i \neq j, \tag{S2}$$

where $\mu_{ij}\big(t, X(t)\big)$ is called a per-capita rate or a unit rate. Flows into the system require special treatment since $X_i(t)$ in (S2) is not defined for $i = \bullet$. Instead, we specify

$$dN_{\bullet i}/dt = \mu_{\bullet i}\big(t, X(t)\big). \tag{S3}$$

This is the the interpretation and implementation used for Model 2 in our study.

S1.2   Simple Markov counting system interpretation

A continuous time Markov chain can be specified via its infinitesimal transition probabilities. A basic approach to this is to define

$$\begin{aligned}
\mathbb{P}\big[N_{ij}(t+\delta) - N_{ij}(t) = 0 \,|\, X(t)\big] &= 1 - \delta \mu_{ij}\big(t, X(t)\big) + o(\delta), \tag{S4} \\
\mathbb{P}\big[N_{ij}(t+\delta) - N_{ij}(t) = 1 \,|\, X(t)\big] &= \delta \mu_{ij}\big(t, X(t)\big) + o(\delta), \tag{S5}
\end{aligned}$$

2

for $i \in 1{:}c$ and $j \in 1{:}c \cup \{\bullet\}$ with $i \neq j$. As with the ODE case, we need special attention for flows into the system, and we define

$$\mathbb{P}\big[N_{\bullet i}(t+\delta) - N_{\bullet i}(t) = 0 \,\big|\, X(t)\big] \;=\; 1 - \delta\mu_{\bullet i}\big(t, X(t)\big) + o(\delta), \qquad (S6)$$

$$\mathbb{P}\big[N_{\bullet i}(t+\delta) - N_{\bullet i}(t) = 1 \,\big|\, X(t)\big] \;=\; \delta\mu_{\bullet i}\big(t, X(t)\big) + o(\delta). \qquad (S7)$$

Together with the initial conditions $X(0)$, equations (S4)–(S7) define a Markov chain. Each flow is a simple counting process, meaning a non-decreasing integer-valued process that only has jumps of size one. We therefore call the Markov chain a simple Markov counting system (SMCS). The infinitesimal mean of every flow is equal to its infinitesimal variance (Bretó and Ionides, 2011) and so an SMCS is called equidispersed. We note that the special case of Model 1 used by Lee et al. (2020a) (with $\sigma_{\mathrm{proc}} = 0$) is an SMCS. To permit more general mean-variance relationships for a Markov counting system, we must permit jumps of size greater than one. The utility of overdispersed models, where the infinitesimal variance of the flow exceeds the infinitesimal mean, has become widely recognized (Stocks et al., 2020; He et al., 2010).

S1.3   Overdispersed Markov counting system interpretation

Including white noise in the rate function enables the possibility of an overdispersed Markov counting system (Bretó and Ionides, 2011; Bretó et al., 2009; He et al., 2010). Since rates should be non-negative, Gaussian noise is not appropriate and gamma noise is a convenient option that has found various applications (Romero-Severson et al., 2015; Subramanian et al., 2020). Specifically, we consider a model given by

$$\mu_{ij}\big(t, X(t)\big) = \bar{\mu}_{ij}\big(t, X(t)\big)\, d\Gamma_{ij}(t)/dt, \qquad (S8)$$

where $\Gamma_{ij}(t)$ is a stochastic process having independent gamma distributed increments, with

$$\mathbb{E}\big[\Gamma_{ij}(t)\big] = t, \quad \mathrm{Var}\big[\Gamma_{ij}(t)\big] = \sigma_{ij}^2 t. \qquad (S9)$$

Formally interpreting the meaning of (S8) is not trivial, and we do so by defining the solution of (S8) to be the limit of an Euler scheme. Therefore, the numerical scheme in Sec. S2 can be taken as a definition of the meaning of (S8). The Markov chain defined by the limit of this Euler scheme as the step size decreases is an overdispersed Markov counting system, with the possibility of instantaneus jumps of size greater than one (Bretó and Ionides, 2011).

S2   Numerical solutions to compartment models

Models may be fitted and their implications assessed via numerical solutions (i.e., simulations) from the model equations. All the analyses we consider have this simulation-based property, known as plug-and-play or equation-free or likelihood-free. The numerical solutions to the model are arguably of more direct scientific interest than the exact solutions to the postulated equations. For ODE models, numerical methods are well studied and a standard numerical solution package such as `deSolve` in `R` is adequate for our purposes. For SMCS and ODMCS models, exact schemes are feasible when the number of events is small, which may be the case for small populations. However, for applicability to larger populations, we use instead the following Euler scheme. Write δ for an Euler time step, and ΔN_{ij} for the numerical approximation to $N_{ij}(t+\delta) - N_{ij}(t)$ given $X(t)$. For

each i and j in $1:c \cup \{\bullet\}$ with $i \neq j$, we draw independent Gamma distributed noise increments with mean δ and variance $\sigma_{ij}^2 \delta$, denoted using a mean-variance parameterization of the gamma distribution as

$$\Delta \Gamma_{ij} \sim \text{gamma}(\delta, \sigma_{ij}^2 \delta). \tag{S10}$$

In the case of an SMCS model, $\sigma_{ij} = 0$ for all i and j, so we have $\Delta \Gamma_{ij} = \delta$. Then, for $i \neq \bullet$ and $j \neq i$, and writing

$$\mu_{ij} = \bar{\mu}_{ij}\big(t, X(t)\big) \Delta \Gamma_{ij}/\delta, \tag{S11}$$

we calculate transition probabilities

$$p_{ij} = \exp\left\{ -\sum_{k \in 1:c \cup \{\bullet\}} \mu_{ik}\, \delta \right\} \frac{\mu_{ij}}{\sum_{k \in 1:c \cup \{\bullet\}} \mu_{ik}}, \tag{S12}$$

$$p_{ii} = 1 - \sum_{j \neq i} p_{ij}. \tag{S13}$$

These probabilities correspond to competing hazards for every individual in compartment i to transition to some compartment j, interpreting $j = i$ to mean that the individual remains in i. Then, $\big(\Delta N_{i1}, \ldots, \Delta N_{ic}, \Delta N_{i\bullet}\big)$ has the multinomial distribution where $X_i(t)$ individuals are allocated independently to $1:c \cup \{\bullet\}$ with probabilities given by (S12) and (S13). We use the `reulermultinom` function in the `pomp` package to draw from this multinomial distribution.

For the case $i = \bullet$, one can use

$$\Delta N_{\bullet j} \sim \text{poisson}(\mu_{\bullet j}\delta), \tag{S14}$$

an independent Poisson random variable with mean $\mu_{\bullet j}\delta$, as was done in Model 1.

Another common approach is to balance the total number of flows in and out of the compartment, i.e., $\sum_i N_{\bullet i}(t) = \sum_i N_{i\bullet}(t)$, in order to make the model consistent with the known total population, as was done in Models 2 and 3. In this case, we formally model the death rate as a rate of returning to the susceptible class S, and use external transitions from $\bullet$ into S to describe only net population increase.

S3 Initial Values

To perform inference on POMP models, it is necessary to propose an initial density for the latent process $f_{X_0}(x_0; \theta)$. This density is used to obtain initial values of the latent state when fitting and evaluating the model. For each of the models considered in this analysis, the initial conditions are derived by enforcing the model dynamics on reported cholera cases. It is also sometimes necessary to fit some initial value parameters in order to help determine starting values for weakly identifiable compartments. In the following subsections, we mention initial value parameters that were fit for each model.

S3.1 Model 1

For this model, the number of individuals in the Recovered and Asymptomatic compartments are set to zero, but the initial proportion of Infected and Exposed individuals is estimated as initial value parameters ($I(0)$ and $E(0)$, respectively) using the MIF2 algorithm. Finally, the initial proportion of Susceptible individuals S_0 is calculated as $S(0) = 1 - I(0) - E(0)$.

S3.2   Model 2

Model 2 assumes that the initial vales are known and constant, and so no initial value parameters need to be estimated. Starting values for latent state compartments are chosen so as to enforce the model dynamics on the observed number of cases. Specifically, the model sets $I_u(0) = y_u^*(0)/\rho$ for each unit $u \in 1:10$, where $I_u(t)$ is the number of infected individuals in unit u at time t, $y_u^*(t)$ is the reported number of cases, and ρ is the reporting rate.

S3.3   Model 3

We use the reported cases at the start of the pandemic to approximate the number of Asymptomatic, Infectious, and Recovered individuals in each department $u \in 1:U$ using the same approximation as provided in Eq. 34. The susceptible compartment is initialized so that the sum $S_u(0) + I_u(0) + A_u(0) + \sum_k R_{u,k}(0) = \text{population}_u$. The bacteria compartment is then initialized using Eq. (S15):

$$B_u(0) = \big[1 + a\big(\xi_u\big)^r\big] D_i\,\mu_W\big[I_u(0) + \epsilon_W A_u(0)\big], \tag{S15}$$

where $\xi_u \in (0,1)$ is an initial value parameter that allows some flexibility in determining the initial state of the bacteria compartment.

S4   Measurement Models

Each POMP requires specification of a measurement model, which is a statistical description of how observations on the system are obtained. In general, we used the same measurement models that were reported by Lee et al. (2020a).

S4.1   Model 1

In this model, the advantage afforded by vaccination is an increased probability that an infection is asymptomatic. Therefore, under the assumptions of this model, all reported cases are assumed to be a fraction of individuals that transition from the exposed to the infected compartment, as noted in Eq. (S16):

$$Y_n \mid \Delta N_{EI}(n) = z(n) \sim \text{NB}\left(\rho z(n), \psi\right), \tag{S16}$$

where Y_n is the reported cholera cases at time $n \in 1:N$ and $\Delta N_{EI}(n)$ is the sum total of individuals across vaccination compartment z who moved from compartment E_z to I_z since observation $n-1 \in 0:N-1$, and $\text{NB}\left(\rho z, \psi\right)$ is the negative binomial distribution with mean ρz and variance $\rho z\big(1+\frac{\rho z}{\psi}\big)$.

S4.2   Model 2

As mentioned in the main text, Model 2 was fit using reported case counts that were transformed using the natural logarithm. We fit Model 2 using the subplex algorithm in the `subplex` package, using a Gaussian measurement model (Eq. (S19)) on the log transformed cases as the loss function.

$$\log\left(Y_{u,n} + 1\right) \mid \Delta N_{EI}(n) = z(n) \sim \text{N}\left(\log\left(\rho z(n) + 1\right), \psi^2\right), \tag{S17}$$

where $\Delta N_{EI}(n)$ is the sum total of individuals across vaccination compartment z and unit u who moved from compartment E_{uz} to I_{uz} since observation $n - 1 \in 0:N-1$. Therefore, because

the natural logarithm of observed case counts (plus one, to avoid taking the logarithm of zero) has a normal distribution, $Y_{u,n} + 1$ is assumed to follow a log-normal distribution with log-mean parameter $\mu = \log\left(\Delta N_{EI}(n) + 1\right)$ and log-variance ψ^2. We note that fitting a model with this measurement model is equivalent to fitting using least squares, with $\log(Y_{u,n} + 1)$ as the response variable.

This measurement model differs from that used by Lee et al. (2020a), who fit the model in two stages: epidemic and endemic phases. Although their text and supplement material do not explicitly describe the measurement model used, inspection of the code provided with their submission suggests a change in measurement model between the epidemic and endemic phases. In the file `choleraEqsPublic.py`, Lee et al. (2020a) create several functions, where each function represents a set of coupled differential equations that could potentially be used to model cholera incidence data. Each function returns a vector (or `numpy` array) that represents the change in each state variable for a single time step, including the variable `dC`, which tracks the number of new infections and is used to obtain the reported case counts. Following their comments and code, it appears that the function `choleraEqs10WithoutVaccinationNetwork` was used to describe the dynamics of the epidemic phase, and `choleraEqs11WithoutVaccinationNetwork` was used for the endemic stage (see Sec S5.2 for more details). Because their models were fit using least squares, the code in these functions suggest that the measurement model for the epidemic phase is

$$Y_{u,n} \mid \Delta N_{EI}(n) = z(n) \sim \mathrm{N}\left(\rho z(n), \psi^2\right), \tag{S18}$$

which is similar to our measurement model, the primary difference being that the measurement model is applied to raw case counts rather than log-transformed case counts. The measurement model for the endemic phase modifies the epidemic model by counting both asymptomatically infected (A) and symptomatically infected (I) individuals in the case counts:

$$Y_{u,n} \mid \Delta N_{EI}(n) = z_1(n), \Delta N_{EA}(n) = z_2(n) \sim \mathrm{N}\left(\rho(z_1(n) + z_2), \psi^2\right), \tag{S19}$$

where the notation for $\Delta N_{EA}(n)$ is similar to $\Delta N_{EI}(n)$, described above.

S4.3 Model 3

In this model, reported cholera cases are assumed to stem from individuals who develop symptoms and seek healthcare. Therefore reported cases are assumed to come from an over-dispersed negative binomial model, given the increase in infected individuals:

$$Y_{u,n} \mid \Delta N_{S_{uz}I_{uz}}(t) = z_u(n) \sim \mathrm{NB}\left(\rho z_u(n), \psi\right), \tag{S20}$$

where $\Delta N_{S_{uz}I_{uz}}(n)$ is the number of individuals who moved from compartment S_{uz} to I_{uz} since observation $n - 1 \in 0 : N - 1$.

This measurement model is a minor change from that used by Lee et al. (2020a), which allowed for a change in the reporting rate on January 1st, 2018. The fitted values of the reporting rate—before and after January 2018—were 0.97 and 0.097, respectively. This major change in reporting rate alone could explain why Model 3 of Lee et al. (2020a) failed to predict the eradication of cholera. An overnight change from near perfect to almost non-existent reporting forces the model to explain the observed reduction in reported cases as a decrease in the reporting of cases, rather than a decrease in the prevalence of cholera. This shift was justified by a "change of the case

definition that occurred on January 1st, 2018"; this claim was not cited, and we could find no evidence that such a drastic change in the reporting rate would be warranted. We therefore do not allow a change in reporting rate when fitting Model 3.

S5 Lee et al. (2020) Replication

In this article we claimed that we were able to obtain better fits to the observed data using the same models that were proposed by Lee et al. (2020a). Along with visual comparisons to the data, this claim was supported by comparing likelihoods and AIC values in Table 1. Because model likelihoods were not provided by Lee et al. (2020a), it is necessary to replicate these models in order to obtain likelihood estimates. Here we would like to thank the authors of Lee et al. (2020a), who provided detailed descriptions of their models, which enabled us to build on their work. In the following subsections, we use our R package `haitipkg` to reproduce some of the results of Lee et al. (2020a). This reproduction allows us to estimate the likelihoods of the Lee et al. (2020a) version of Models 1–3, and also provides a demonstration on reproducibility.

S5.1 Model 1 Replication

The model was implemented by a team at Johns Hopkins Bloomberg School of Public Health (hereafter referred to as the Model 1 authors) in the R programming language using the `pomp` package (King et al., 2016). Original source code is publicly available with DOI: 10.5281/zenodo.3360991. Despite having source code available, no point estimates for model parameters were provided by Lee et al. (2020a). According to the supplement materials, this was because model realizations from a single parameter set retained substantial variability, but multiple realizations from a collection of parameter sets resulted in a reasonable visual fit to the data. We are also inclined to believe that the use of multiple parameter values was in part intended to account for parameter uncertainty (as mentioned in our main text), an effort by the Model 1 authors that we applaud. We note, however, that simulations from each of the parameter sets were treated with equal importance when being used to diagnose the model fit and make inference on the system. This practice is problematic given Figures S8 and S9 of the supplement material, which suggest that some parameter sets that were used for inference were several hundred log-likelihood units lower than the best performing sets of parameters. When accounting for parameter uncertainty, one should instead weigh resulting model projections based on the likelihood of the set of parameters that were used to obtain the model realizations, as was done by King et al. (2015).

Not providing a point estimate for model parameters also has the effect of making model reproduction a more difficult task. We therefore rely on the range and median values for each of the final model parameters are provided in Tables S10 and S11 of the supplement, and bivariate relationships between some of the fitted parameters (Figures S8 and S9) in order to replicate their results.

We begin by constructing 300 different parameter sets based on the basic summaries and figures provided by the Model 1 authors. This was primarily done using truncated-bivariate normal distributions, where samples that are drawn outside of the desired range of parameters are re-sampled from the distribution. Because the likelihood surface is complex and almost certainly includes higher than two-level interactions between parameter values, we then perform iterated filtering for the epidemic phase of the data using the 300 different parameter sets as starting points.
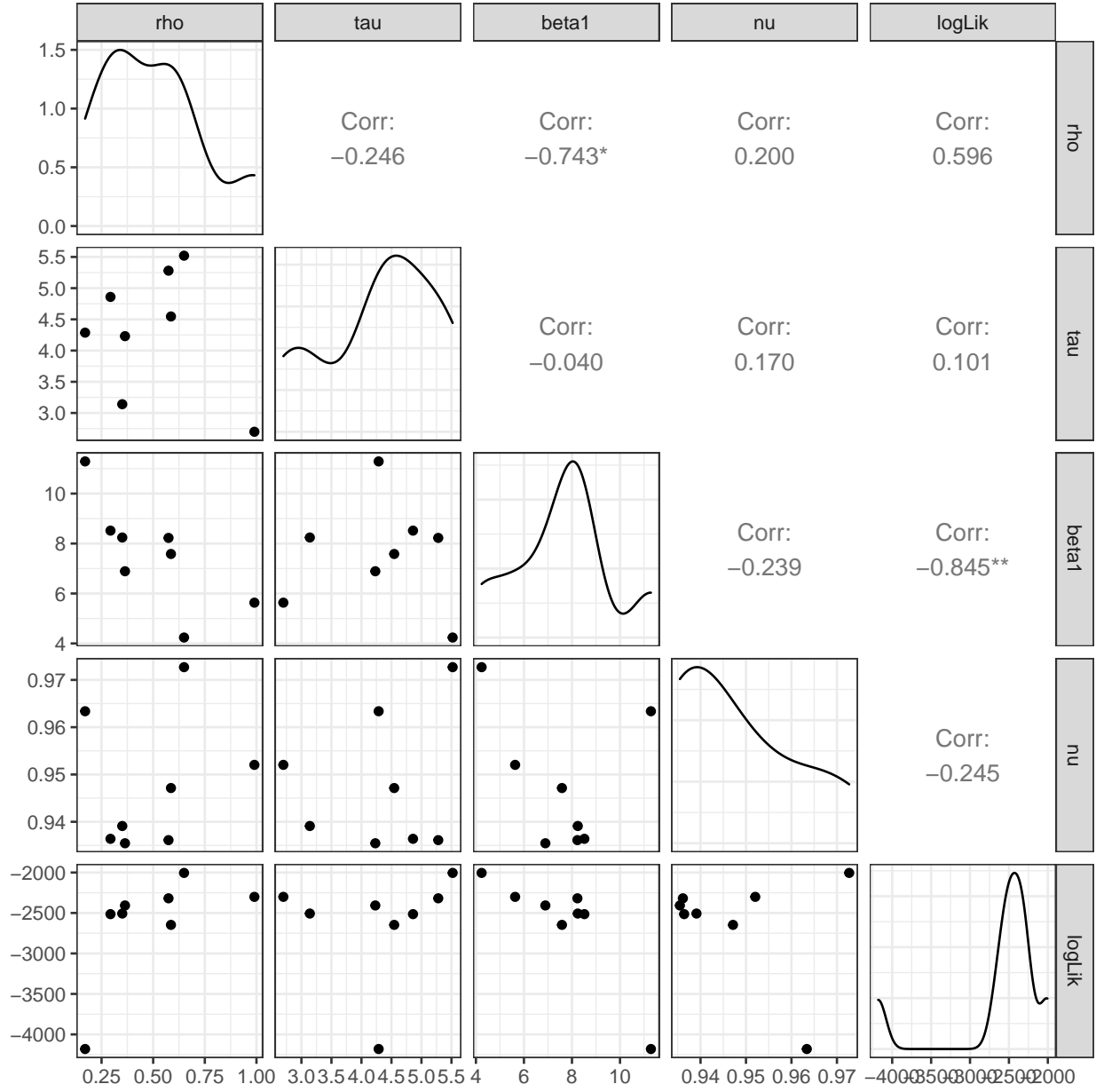
Figure S-1: Compare to Figure S8 of Lee et al. (2020) supplement.

Following the model fitting scheme used by the Model 1 authors, we then use these resulting parameters as starting values for the endemic phase, and refit parameters using MIF2. To do this, we use the same number of particles and MIF iterations that were used by Lee et al. (2020a). The resulting bivariate relations between ρ, τ, β_1 and ν are given in Figure S-2.

Now that we have fit the parameters, we can simulate from the models. The results of these simulations are shown in Figure S-3. While not a perfect replication of the results given by Lee et al. (2020b), the similarities between the model simulations, and the fact that we based our implementation of Model 1 primarily on the source code that was provided, makes us confident that we have been able to obtain a reliable representation of the model described by Lee et al. (2020a).

S5.2   Model 2 Replication

Model 2 was developed by a team that consisted of members from the Fred Hutchinson Cancer Research Center and the University of Florida (hereafter referred to as the Model 2 authors). While Model 2 is the only deterministic model we considered in our analysis, it contains perhaps the most complex descriptions of cholera in Haiti: Model 2 accounts for movement between spatial units; human-to-human and environment-to-human cholera infections; and transfer of water between spatial units based on elevation charts and river flows.

The source code that the Model 2 authors used to generate their results was written in the `Python` programming language, and is publicly available at `10.5281/zenodo.3360857` and its accompanying GitHub repository `https://github.com/lulelita/HaitiCholeraMultiModel ingProject`. In order to perform our analysis in a unified framework, we re-implemented this model in the `R` programming language using the `spatPomp` package (Asfaw et al., 2021), which facilitates the creation of meta-population models. We note that the travel and water matrices used to implement the complex dynamics in Model 2 (Lee et al., 2020b) are not available in either the Zenodo archive or the GitHub repository; instead, we obtained these matrices via personal correspondence with the Model 2 authors. Using these matrices, and the point estimates for model parameters provided by (Lee et al., 2020b), we created trajectories of the cholera dynamics and compared this to available data. These trajectories, shown in Figure S-4, are very similar to the trajectories shown in Figure S15 of Lee et al. (2020b).

There are minor differences between Figure S-4 and Figure S15 of Lee et al. (2020b). While the discrepancy appears minor, the deterministic nature of Model 2 implies that an exact replication of model trajectories should be possible. In this case, these discrepancies may be attributed to model implementation and small differences in model parameters. Details about the measurement models and how latent states were initialized for the epidemic model were not provided by Lee et al. (2020b) and therefore these details must be inferred by looking at the provided source code. According to repository comments, the files `fitInPieces3paramsCleanMay2019Public.py` and `fitInPiecesMuWithFracSusFixedAllInfectionsPublic.py` were used to fit the epidemic and endemic phases of the model respectively, although it is apparent that these exact files were not used to obtain the reported results. These files contain errors that making them impossible to run, and therefore these files cannot be the code that generated the reported model fits[1]. The inability to replicate the results by Lee et al. (2020a) by running the provided source code makes checking

---

[1] One example of why the code cannot be run that the file loads functions from a non-extant file named `choleraEqs.py` in line 13 rather than `choleraEqsPublic.py`.
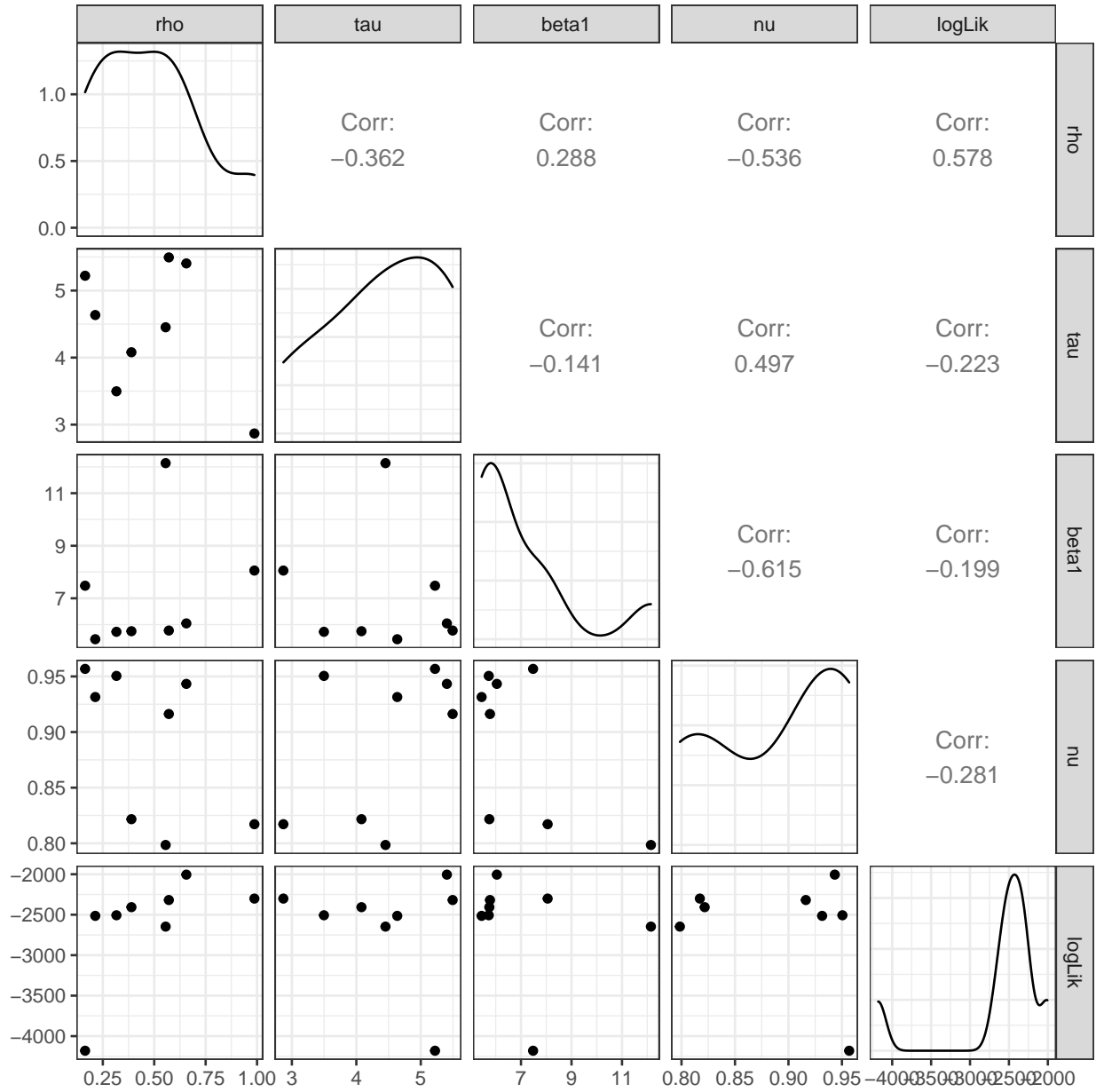
Figure S-2: Bivariate relationships between variables after fitting endemic period. Compare to S9 of Lee et al. (2020) supplement.
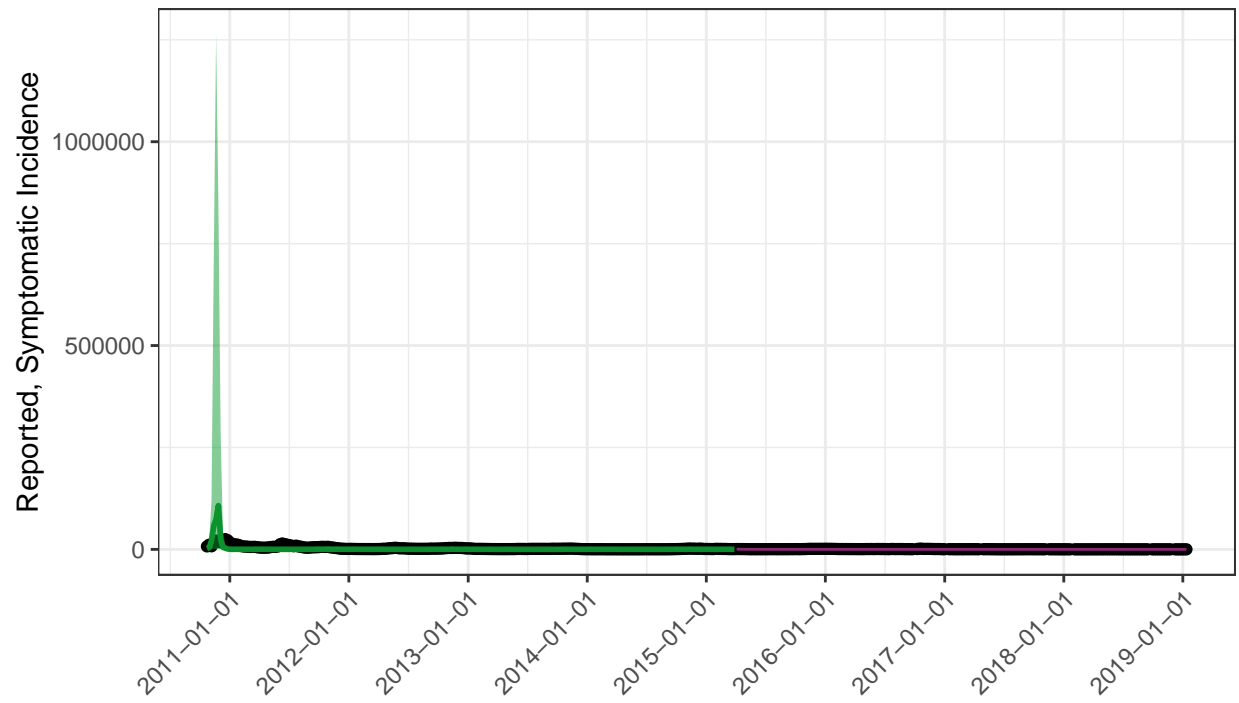
Figure S-3: Simulations from various parameter sets. Simulations from parameter sets with likelihood < -2200 are removed. Compare to Figure S7 of Lee et al. (2020b).
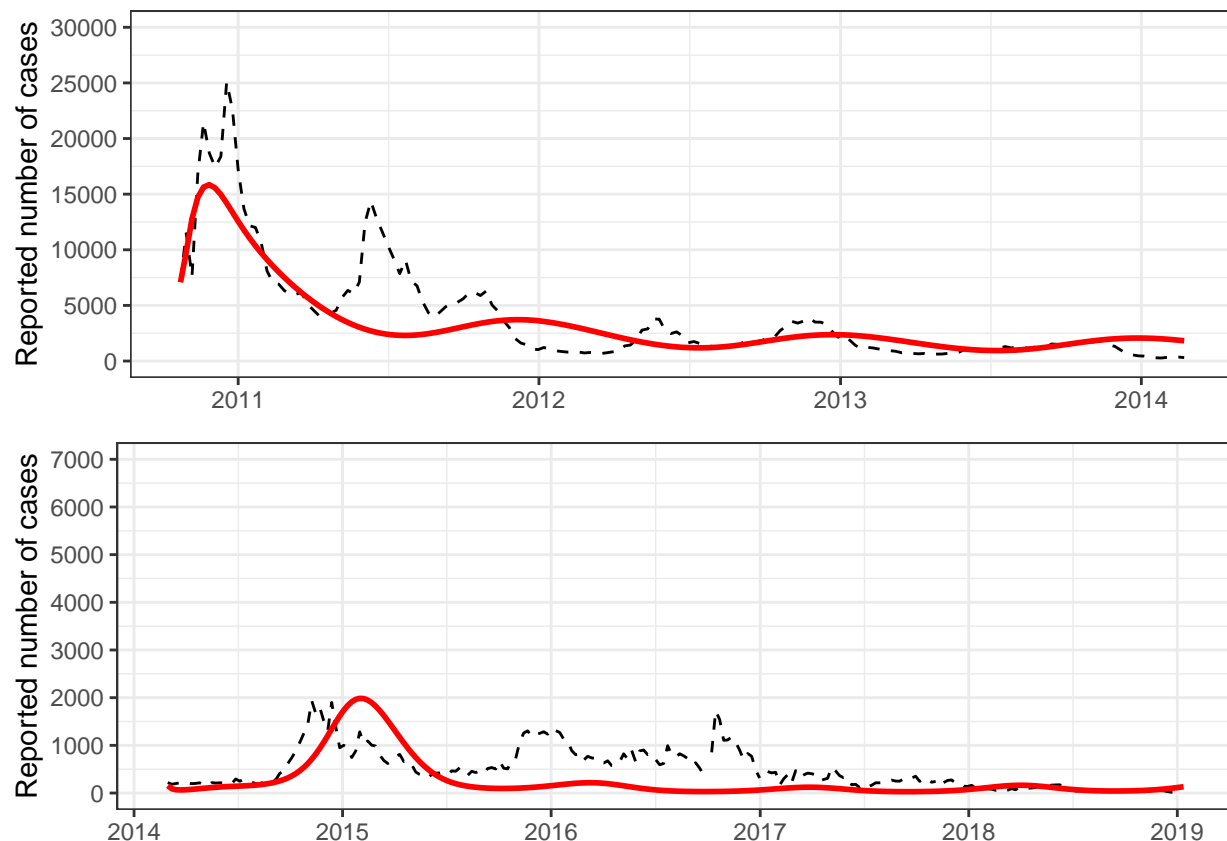
Figure S-4: Model 2 trajectories using the `haitipkg`. Compare to Figure S15 of Lee et al. (2020b).

whether or not a our numeric implementation faithfully represents their results very difficult.

[PROBABLY DELETE THIS NEXT BIT, BUT IT'S USEFUL TO DOCUMENT IT FOR NOW...] One concern that arises when inspecting the files `fitInPieces3paramsCleanMay2019Public.py` and `fitInPiecesMuWithFracSusFixedAllInfectionsPublic.py` is that the output of these files (which contains the estimated parameters) was not referenced/used in either the file that generates the sensitivity analysis or the file that generates the model simulations; instead, alternative (non-extant) files with similar names are loaded, suggesting parameters that were used to generate the final results were not a direct result of the estimated parameters. Furthermore, inspection of the script `simulateHaitiFullTimeInPiecesAllVaccinationScenariosSingleParameterVectorAllInfectionsPubl` which is used to obtain simulations for each of the vaccination scenarios—results in a number of concerns. First, the script uses parameters from the pickle file `leastSquaresDataUpTo2019/fitEpidemicPiece_resul`, which only appears in the repository as a commented out line of code in the file `generateSetsOfParametersForSens` suggesting that the set of parameters used to simulate each vaccination scenario was not the most recent set of parameters generated by the sensitivity analysis. Second, the script appears to use the set of differential equations from the function `choleraEqs11WithVaccinationNetwork` for the epidemic phase, even though parameter values for this phase were estimated using `choleraEqs10WithVaccinationNetwork`. It is possible, however, that we simply are interpreting the code incorrectly and that these concerns are unwarranted. Furthermore, because the provided code is non-functional, it is possible that the

code that was actually used to obtain the reported results does not include these potential errors. This highlights the importance of providing the exact source code that was used to obtain the reported results of any analysis.

Another potential explanation for the discrepancy between our simulations from Model 2 and those of Lee et al. (2020a) is that the parameters that we used are only approximately the same as those used by Lee et al. (2020b). For example, the parameters β, β_W (See Table S-1) had reported values of 9.9×10^{-7} and 4.03×10^{-2}, respectively (Table S13 of Lee et al. (2020b)), but were actually fit to data and therefore likely had values that were far more precise. Additionally, our implementation of Model 2 used a time scale of years and many of the parameters were reported on a weekly scale, so small differences may result due to unit conversions. The collective effect of these small differences in model parameters likely will result in differences in model trajectories. This issue could have been mitigated if the saved files containing estimated model parameters were included as part of the code submission.

S5.3   Model 3 Replication

Model 3 was developed by a team of researchers at the Laboratory of the Swiss Federal Institute of Technology in Lausanne, hereafter referred to as the Model 3 authors. The code that was originally used to implement Model 3 is archived with the DOI: `10.5281/zenodo.3360723`, and also available in the public GitHub repository: `jcblemai/haiti-mass-ocv-campaign`. Because the code was made publicly available, and final model parameters were reported in the supplementary material of Lee et al. (2020a), we were able to reproduce Model 3 by directly using the source code. In Fig. S-5, we plot simulations from this model. This figure should be compared to Figure S18 of Lee et al. (2020a). We note that slight differences may be accounted for due to variance in the model simulations and the difference in programming language used to produce the figure.

S6   Translating to Lee et al. (2020a) notation

Since the models of Lee et al. (2020a) were developed independently, the choice of notation varies inconsistently between models. For our reanalysis, we rename parameters to provide a unified notation facilitating comparison between models. Table S-1 maps this notation back to the original notations, for reference.

Parameter	Our Notation	Lee et al. (2020a)		
		1	2	3
Reporting Rate	ρ	ρ	ρ	ϵ_1, ϵ_2
Mixing Coefficient	ν	ν	—	—
Measurement Over-Dispersion	ψ	τ	—	p
Birth Rate	μ_S	μ	—	—
Natural Mortality Rate	δ	δ	—	μ
Cholera Mortality Rate	δ_C	—	—	α
Latent Period	$1/\mu_{EI}$	$1/\sigma$	$1/\gamma_E$	—
Recovery Rate	μ_{IR}	γ	γ	γ
Loss of Immunity	μ_{RS}	α	σ	ρ
Symptomatic Ratio	f	$1 - \theta_0$	k	σ
Asymptomatic Relative Infectiousness	ϵ	κ	red_β	—
Human-to-Water Shedding	μ_W	—	μ	θ_I
Asymptomatic Relative Shedding	ϵ_W	—	red_μ	θ_A/θ_I
Seasonal Amplitude	a	—	α_s	λ
Transmission	β	β	β	c
Water-to-Human	β_W	—	β_W	β
Bacteria Mortality	δ_W	—	δ	μ_β
Vaccination Efficacy	θ	θ_{vk}	$\theta_1, \theta_2, \theta_{1_5}, \theta_{2_5}$	η_{1d}, η_{2d}
Process Over-dispersion	σ_{proc}	—	—	σ_w

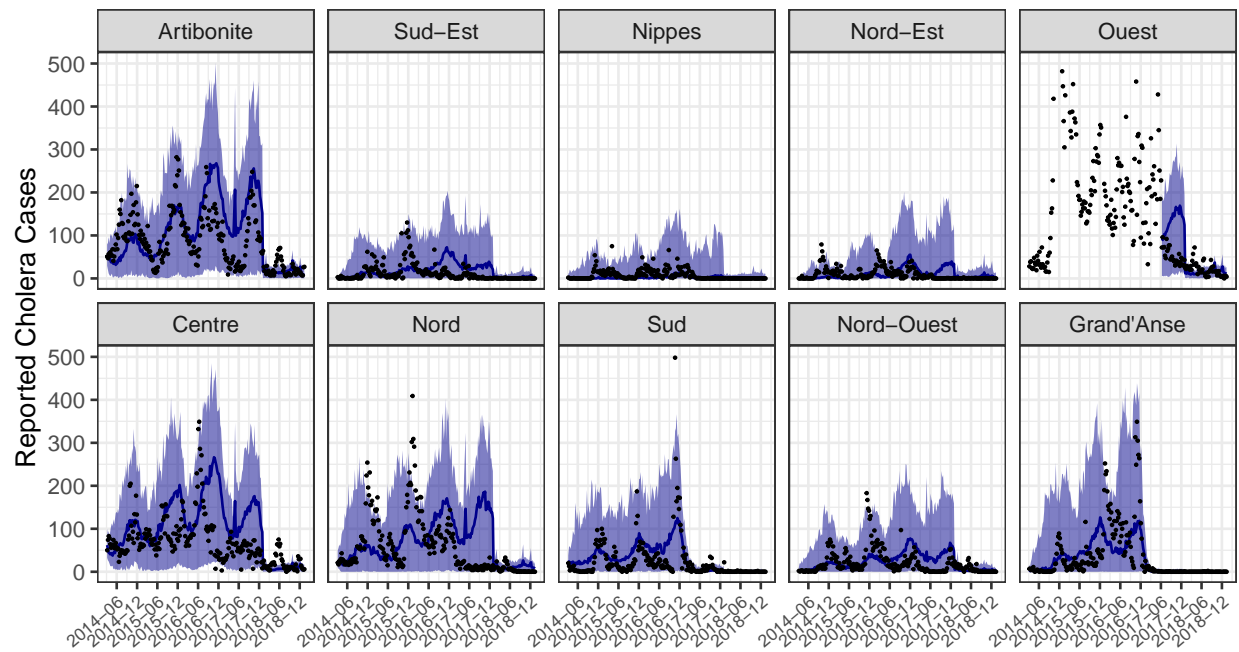Table S-1: Translations between our common notation and notation used by Lee et al. (2020a)

Figure S-5: Simulations from Model 3. Compare to Figure S18 of Lee et al. (2020a).

Supplementary References

Asfaw, K., Ionides, E. L., and King, A. A. (2021). `spatPomp`: R package for statistical inference for spatiotemporal partially observed Markov processes. `https://github.com/kidusasfaw/spatPomp`.

Bhadra, A., Ionides, E. L., Laneri, K., Pascual, M., Bouma, M., and Dhiman, R. C. (2011). Malaria in Northwest India: Data analysis via partially observed stochastic differential equation models driven by Lévy noise. *Journal of the American Statistical Association*, 106:440–451.

Bretó, C., He, D., Ionides, E. L., and King, A. A. (2009). Time series analysis via mechanistic models. *Annals of Applied Statistics*, 3:319–348.

Bretó, C. and Ionides, E. L. (2011). Compound Markov counting processes and their applications to modeling infinitesimally over-dispersed systems. *Stochastic Processes and their Applications*, 121:2571–2591.

Bretó, C., Ionides, E. L., and King, A. A. (2020). Panel data analysis via mechanistic models. *Journal of the American Statistical Association*, 115(531):1178–1188.

Domeyer, J. E., Lee, J. D., Toyoda, H., Mehler, B., and Reimer, B. (2022). Driver-pedestrian perceptual models demonstrate coupling: Implications for vehicle automation. *IEEE Transactions on Human-Machine Systems*, pages 1–10.

He, D., Ionides, E. L., and King, A. A. (2010). Plug-and-play inference for disease dynamics: Measles in large and small towns as a case study. *Journal of the Royal Society Interface*, 7:271–283.

Ionides, E. L., Ning, N., and Wheeler, J. (2022). An iterated block particle filter for inference on coupled dynamic systems with shared and unit-specific parameters.

King, A. A., Domenech de Cellès, M., Magpantay, F. M., and Rohani, P. (2015). Avoidable errors in the modelling of outbreaks of emerging pathogens, with special reference to ebola. *Proceedings of the Royal Society B: Biological Sciences*, 282(1806):20150347.

King, A. A., Nguyen, D., and Ionides, E. L. (2016). Statistical inference for partially observed Markov processes via the R package pomp. *Journal of Statistical Software*, 69:1–43.

Lee, E. C., Chao, D. L., Lemaitre, J. C., Matrajt, L., Pasetto, D., Perez-Saez, J., Finger, F., Rinaldo, A., Sugimoto, J. D., Halloran, M. E., Longini, I. M., Ternier, R., Vissieres, K., Azman, A. S., Lessler, J., and Ivers, L. C. (2020a). Achieving coordinated national immunity and cholera elimination in Haiti through vaccination: A modelling study. *The Lancet Global Health*, 8(8):e1081–e1089.

Lee, E. C., Chao, D. L., Lemaitre, J. C., Matrajt, L., Pasetto, D., Perez-Saez, J., Finger, F., Rinaldo, A., Sugimoto, J. D., Halloran, M. E., Longini, I. M., Ternier, R., Vissieres, K., Azman, A. S., Lessler, J., and Ivers, L. C. (2020b). Supplement to: Achieving coordinated national immunity and cholera elimination in Haiti through vaccination: A modelling study. *The Lancet Global Health*, 8(8):e1081–e1089.

Ning, N. and Ionides, E. L. (2021). Iterated block particle filter for high-dimensional parameter learning: Beating the curse of dimensionality.

Ranjeva, S., Subramanian, R., Fang, V. J., Leung, G. M., Ip, D. K., Perera, R. A., Peiris, J. M., Cowling, B. J., and Cobey, S. (2019). Age-specific differences in the dynamics of protective immunity to influenza. *Nature communications*, 10(1):1660.

Ranjeva, S. L., Baskerville, E. B., Dukic, V., Villa, L. L., Lazcano-Ponce, E., Giuliano, A. R., Dwyer, G., and Cobey, S. (2017). Recurring infection with ecologically distinct HPV types can explain high prevalence and diversity. *Proceedings of the National Academy of Sciences*, page 201714712.

Rebeschini, P. and van Handel, R. (2015). Can local particle filters beat the curse of dimensionality? *The Annals of Applied Probability*, 25(5):2809–2866.

Romero-Severson, E., Volz, E., Koopman, J., Leitner, T., and Ionides, E. (2015). Dynamic variation in sexual contact rates in a cohort of HIV-negative gay men. *American Journal of Epidemiology*, 182:255–262.

Stocks, T., Britton, T., and Höhle, M. (2020). Model selection and parameter estimation for dynamic epidemic models via iterated filtering: application to rotavirus in germany. *Biostatistics*, 21(3):400–416.

Subramanian, R., Romeo-Aznar, V., Ionides, E., Codeço, C. T., and Pascual, M. (2020). Predicting re-emergence times of dengue epidemics at low reproductive numbers: Denv1 in rio de janeiro, 1986–1990. *Journal of the Royal Society Interface*, 17(167):20200273.

Wale, N., Jones, M. J., Sim, D. G., Read, A. F., and King, A. A. (2019). The contribution of host cell-directed vs. parasite-directed immunity to the disease and dynamics of malaria infections. *Proceedings of the National Academy of Sciences*, 116(44):22386–22392.